

## Hydrodynamic Parameterization of NA44 Data on Kaon and Pion Correlations and Spectra

T. Csörgő<sup>1,2a</sup> and B. Lörstad<sup>3b</sup>

<sup>1</sup> Department of Physics, Columbia University  
538 W 120th St New York, N. Y. 10027

<sup>2</sup> KFKI Research Institute for Particle and Nuclear Physics  
H-1525 Budapest 114, POB 49, Hungary

<sup>3</sup> Physics Department, Lund University  
S-221 00 Lund, POB 118, Sweden

*Received 30 June 1996*

**Abstract.** An analytically calculable model [1] has been proposed recently for the simultaneous description of particle spectra and correlations, which is able to explain in a natural manner the  $m_t$  scaling of the radius parameters of the Bose–Einstein correlation functions. We present here *preliminary* results on fitting this model to data sampled by NA44 collaboration in central S + Pb reactions at CERN SPS, which indicate that both pions and kaons freeze-out at a surprisingly low temperature of  $T \simeq 108$  MeV.

### 1. Introduction

Recently there has been much interest in the measurement and the calculation of the Bose–Einstein correlation functions (BECFs) and those of the invariant momentum distributions (IMDs) for rapidly expanding systems with flow and temperature profiles. The expansion may result in strong correlations between space-time and momentum space variables implying that the Bose–Einstein correlations are in general not measuring the geometrical sizes of big and expanding finite systems. The geometrical sizes play an important role in the description of the invariant momentum distributions. That is why a simultaneous fit of IMDs and BECFs gives good constraints on the parameters of the model.

We will discuss an attempt to fit simultaneously the data of S+Pb interactions analysed by the NA44 collaboration [2]. They showed an unexpected, scaling behaviour for the radii parameters of the BECF,  $R_{side}$ ,  $R_{out}$  and  $R_{long}$ . These parameters turned out to be proportional to  $1/\sqrt{m_t}$ , where  $m_t$  is the mean transverse mass of the identical particle pair. The same proportionality factor was valid for both pions and kaons. The NA44 collaboration has also measured the IMDs for the same S+Pb interactions using similar trigger conditions. Data are not yet fully

0231-4428/96/ \$ 5.00

Akadémiai Kiadó, Budapest, 1996

normalized but that is not so serious for our purpose as we will only fit the shape of the IMD anyway. We have two reasons to only take the shape into account:

(i) The slightly different trigger conditions for data sampled to measure IMD and for BECF might give slightly different normalizations but the shape is observed to be unaffected [3].

(ii) The expansion model is applicable only to the central finite core creating particles, not to all particles measured. This core is characterized by hydrodynamic, collective behaviour and small lengths of homogeneity. This is in contrast to the halo, created by the decay products of long-lived resonances, which is characterized by a free streaming and decay of these resonances and correspondingly with large lengths of homogeneity proportional to the decay time of the long-lived resonances, [4]. The  $\lambda$  parameter which measures the strength of the correlation gives a handle to estimate the fraction of particles which are produced in the core [5, 4]. When  $\lambda$  is independent of  $m_t$  the IMD of the core particles is proportional to the IMD of all particles measured. The S+Pb data show an approximately  $m_t$  independent  $\lambda$  parameter,  $\lambda_{\pi^+} = 0.56 \pm 0.02$  and  $0.55 \pm 0.02$  at the quite different transverse momenta of 150 MeV and 450 MeV, respectively.

We will shortly present the model of the core, present the results of a fit to three sets of IMDs and the corresponding radii measurements using (i) an analytical approximation and (ii) a numerical integration method. We will summarize with some conclusions.

## 2. A Model of the Core

For central heavy ion collisions at high energies the beam or  $z$  axis becomes a symmetry axis. Since the initial state of the reaction is axially symmetric and the equations of motion do not break this pattern, the final state must be axially symmetric, too. However, in order to generate the thermal length scales in the transverse directions, the flow field must be either three-dimensional, or the temperature must have significant gradients in the transverse directions. Furthermore, the local temperature may change during the the duration of the particle emission either because of the re-heating of the system caused by the hadronization and/or intensive rescattering processes or the local temperature may decrease because of the expansion and the emission of the most energetic particles from the interaction region. We consider the following emission function for high energy heavy ion reactions as a model of the core:

$$S_c(x, p) d^4x = \frac{g}{(2\pi)^3} \frac{d^4\Sigma^\mu(x) p_\mu}{\exp\left(\frac{u^\mu(x) p_\mu}{T(x)} - \frac{\mu(x)}{T(x)}\right) - 1}, \quad (1)$$

where  $d^4\Sigma^\mu(x) p_\mu$  describes the flux of particles through a finite layer of freeze-out hypersurfaces. We assume that this layer is parameterized by  $\tau = \sqrt{t^2 - z^2}$  where

the random variable  $\tau$  is characterized by a probability distribution, such that

$$d^4\Sigma^\mu(x)p_\mu = m_t \cosh[\eta - y] H(\tau) d\tau \tau_0 d\eta dr_x dr_y, \quad (2)$$

where the finite duration is modelled by  $H(\tau) \propto \exp(-(\tau - \tau_0)^2/(2\Delta\tau^2))$ . Here  $\tau_0$  is the mean emission time,  $\Delta\tau$  is the duration of the emission in (proper) time. The four-velocity and the local temperature and density profile of the expanding matter is given by

$$u(x) = \left( \cosh[\eta] \cosh[\eta_t], \sinh[\eta_t] \frac{r_x}{r_t}, \sinh[\eta_t] \frac{r_y}{r_t}, \sinh[\eta] \cosh[\eta_t] \right), \quad (3)$$

$$\frac{1}{T(x)} = \frac{1}{T_0} \left( 1 + a^2 \frac{r_t^2}{2\tau_0^2} \right) \left( 1 + d^2 \frac{(\tau - \tau_0)^2}{2\tau_0^2} \right), \quad \sinh[\eta_t] = b \frac{r_t}{\tau_0}, \quad (4)$$

$$\frac{\mu(x)}{T(x)} = \frac{\mu_0}{T_0} - \frac{r_x^2 + r_y^2}{2R_G^2} - \frac{(\eta - y_0)^2}{2\Delta\eta^2}, \quad (5)$$

where  $\mu(x)$  is the chemical potential and  $T(x)$  is the local temperature characterizing the particle emission.

Note that in Ref. [1] we have considered the Boltzmann approximation to the emission function given by the present eqs. (1 - 5). Thus the results obtained in Ref. [1] correspond to Boltzmann approximations. Here we indicate some new analytic results for the single particle inclusive spectra which are obtained *without* the full Boltzmann approximation.

The emission function of eqs. (1 - 5) corresponds to a *longitudinally expanding, finite* system, with *transverse and temporal temperature profile* and with a linear *transverse flow* velocity profile. The decrease of the temperature in the transverse direction is controlled by the parameter  $a$ , while the strength of the transverse flow is controlled by the parameter  $b$ . The parameter  $d$  controls the strength of the change of the local temperature during the course of particle emission. This parameterization corresponds to a Gaussian approximation of the local flow, inverse temperature and chemical potential profiles, as discussed in detail in Ref. [1]. For the case of  $a = d = 0$  we recover a model also discussed in Ref. [6], while for the case of  $d = 0$  the model of Ref. [7] is reproduced, while for  $b = d = 0$  we obtain a version of a model proposed in Ref. [8].

Using a saddle point approximation similar to the one presented in Ref. [1], but keeping the Bose-Einstein form of the emission function, we find that the IMD of the particles produced from the core plus the halo can be expressed as:

$$\frac{d^2n}{dy dm_t^2} = \frac{1}{\sqrt{\lambda_*}} \frac{d^2n_c}{dy dm_t^2}, \quad (6)$$

$$\frac{1}{\pi} \frac{d^2n_c}{dy dm_t^2} = \frac{g}{(2\pi)^3} V_*(x_s) \frac{p^\mu n_\mu(x_s)}{\exp\left(\frac{u^\mu(x_s)p_\mu}{T(x_s)} - \frac{\mu(x_s)}{T(x_s)}\right) - 1}. \quad (7)$$

This result can be considered new as compared to the ones presented in Ref. [1], but applying a Boltzmann approximation to this result reproduces the expressions given in Ref [1]. Parts of this expression are explained piece by piece below. The intercept parameter  $\lambda_*$ , which relates the total number of particles to the number of particles originating from the core, is the effective intercept parameter of the Bose–Einstein correlation function. The intercept parameter  $\lambda_*$  is not prescribed by the model, it has to be taken from the *correlation* measurements. Note that  $\lambda_*$  is in general rapidity and transverse mass dependent and thus may depend on the kinematic region where the data are determined. The effective volume factor  $V_*(x_s)$  measures the invariant volume element of the particle emission at the time of the last interactions. *This factor can be very strongly  $m_t$  dependent, and its possible  $m_t$  dependence should be taken into account in the future data analysis* [1]. This invariant, effective volume factor is related to the HBT radius parameters [1] as

$$V_*(x_s) = (2\pi\tau_0^2\Delta\eta_*^2)^{\frac{1}{2}} (2\pi R_*^2) \frac{\Delta\tau_*}{\Delta\tau}. \quad (8)$$

The effective source dimensions in the transverse, longitudinal and temporal directions were obtained in Boltzmann approximation in Ref. [1] as

$$\frac{1}{R_*^2} = \frac{1}{R_G^2} + \frac{1}{R_T^2} \cosh[\eta_s], \quad (9)$$

$$\frac{1}{\Delta\eta_*^2} = \frac{1}{\Delta\eta^2} + \frac{1}{\Delta\eta_T^2} \cosh[\eta_s] - \frac{1}{\cosh[\eta_s]^2}, \quad (10)$$

$$\frac{1}{\Delta\tau_*^2} = \frac{1}{\Delta\tau^2} + \frac{1}{\Delta\tau_T^2} \cosh[\eta_s], \quad (11)$$

$$R_T^2 = \frac{\tau_0^2}{a^2 + b^2} \frac{T_0}{m_t}, \quad (12)$$

$$\Delta\eta_T^2 = \frac{T_0}{m_t}, \quad \text{and} \quad \Delta\tau_T^2 = \frac{\tau_0^2}{d^2} \frac{T_0}{m_t}. \quad (13)$$

while the Cooper–Frye flux factor contains  $n^\mu$ , the normal-pointing unit vector of the hypersurface family  $d^4\Sigma^\mu(x)$ . This Cooper–Frye flux factor is given by

$$p^\mu n_\mu(x_s) = m_t \cosh[\eta_s] \quad (14)$$

In the present status report we do not yet consider the effects of Bose–Einstein statistics on the saddle-point and on the radius parameters of the Bose–Einstein correlation functions. In *Boltzmann approximation*, the saddle point  $x_s$  is characterized by  $\tau_s = \tau_0$ ,  $\eta_s = (y_0 - y)/[1 + \Delta\eta^2(m_t/T_0 - 1)]$ ,  $r_{x,s} = \beta_t b R_*^2(\eta_s) m_t / (\tau_0 T_0)$  and  $r_{y,s} = 0$ , if the saddle-point equations can be *linearized* in the LCMS [9] around  $r_x = 0$ . For the NA44 experiment, the mid-rapidity is located at  $y_0 = 3$ .

The same length scales, which determine the effective, invariant volume factor,  $V_*$ , shall determine the radius parameters of the BECF. These length scales, indexed by subscript  $*$ , are the homogeneity lengths in the considered spatial or temporal directions. From the above expressions it is clear that they are determined by an interplay of the geometrical scales,  $R_G$ ,  $\Delta\eta$ , and  $\Delta\tau$  and the so-called thermal scales,  $R_T$ ,  $\Delta\eta_T$ , and  $\Delta\tau_T$ , which are indexed with subscript  $T$  and stem from the Boltzmann factor  $\exp[p^\mu u_\mu(x_s)/T(x_s)]$ . In Boltzmann approximation, utilizing a solution of the linearized saddle point equations [1] one obtains in the mid-rapidity region, for  $y = y_0$ , in the LCMS system [9]:

$$R_{side}^2 = R_*^2, \quad (15)$$

$$R_{out}^2 = R_*^2 + \beta_t^2 \Delta\tau_*^2, \quad (16)$$

$$R_L^2 = \tau_0^2 \Delta\eta_*^2. \quad (17)$$

The BECF can be expressed as

$$C(Q; K) = 1 + \lambda_* \exp(-R_{side}^2 Q_{side}^2 - R_{out}^2 Q_{out}^2 - R_L^2 Q_L^2 - 2R_{out,L}^2 Q_{out} Q_L) \quad (18)$$

For the NA44 data, which are sampled in the central region,  $y \approx 3$ , we have  $R_{out,L}^2 \approx 0$ . A more detailed discussion on the HBT radii was given in Ref. [1].

From the above expressions one can figure out that the radius parameters in general may have complicated dependence on the rapidity and on the transverse mass of the particle pairs. This is partly due to the rapidity and transverse mass dependence of the  $\eta_s = \eta_s^{LCMS}$  variable, the cross-term generating hyperbolic mixing angle [1] defined in the LCMS frame, and partly due to the simultaneous presence of  $m_t$  dependent and  $m_t$  independent terms in eqs. (12 - 13). We see also, that all radii parameters may be proportional to  $1/\sqrt{m_t}$  in the case when the total size and time spread of the particle emission are much larger than the corresponding thermal sizes,  $R_T$ ,  $\Delta\eta_T$  and  $\Delta\tau_T$ , respectively.

There is no a priori reason to assume that  $S_\pi(x, p) = S_K(x, p)$  i.e. that the emission functions have the same form for pions ( $\pi$ ) and kaons ( $K$ ). Freeze-out arguments are based on the estimated value of the hadronic cross-sections and the pions have larger cross-sections than the kaons. On this basis, one would expect that pions will freeze-out later, from a larger volume, than the kaons.

Our results on the parameters of the two-particle correlation function indicate, that even if the geometrical radii for the pion emission function and the kaon emission function were different, they may play only a minor role if they are sufficiently large as compared to the thermal length-scales. Thus the parameters of the Bose-Einstein correlation function may obey an  $m_t$  scaling even if the emission functions of the various hadronic pieces were different [10].

The radii parameters are mainly sensitive to the smallest of the 2 scales present, in contrast to the IMDs which are sensitive to the biggest of the scales. The model is discussed in detail in Ref. [1], where the spectrum has been calculated in a Boltzmann approximation, allowing for a detailed analysis of the influence

of the thermal and geometrical length scales on the rapidity width and the slope parameter of the momentum distribution.

### 3. Fitting Data with Analytical Formulas and Using Numerical Integrations

In the previous section, we have discussed some new features of the Bose-Einstein statistics on the momentum distribution obtained in the saddle-point approximation. In this section, we present a status report about fitting the *Boltzmann* approximations to eq. (1) to NA44 data, both analytically and numerically. Our fitted formulas thus are not taken from the previous chapter, but from Ref. [1], which corresponds to an improved saddle-point approximation to the Boltzmann-approximated emission function. Work is in progress to study the effects of Bose-Einstein statistics on the analytic and numerical fitting of these NA44 data. In a qualitatively similar analysis of the NA49 data the effects arising from the Bose-Einstein statistics were reported to be significantly influencing the quality of the fit [16].

Thus we have tested the model of ref. [1] by a  $\chi^2$ -fit to the NA44 data on the parameters of the kaon and pion BECF as well as on the kaon and pion IMD. In the fit, the data points for the kaon and pion spectrum did not include yet the systematic errors, which were first estimated in Refs. [11, 12]. We have fitted the analytical results for the spectrum obtained in a Boltzmann approximation using the modified saddle point method, as described in Ref. [1].

Our results are still preliminary because of the following reasons:

- i)* At the time of the fitting the systematic errors on the pion and kaon IMD were not yet available, which resulted in underestimated errors on the spectrum. The small errors in turn imposed a too strong requirement on the fitting, and increased the relative weight of the spectrum data points with respect to the radius parameters, for which both the systematic and the statistical errors were determined experimentally. As a consequence, the preliminary results discussed below underestimate the errors of the fitted parameters.
- ii)* We are currently developing a method which supposedly will allow us to analytically estimate the errors made when the saddle-point integrations are carried out. This could be potentially very helpful to restrict the domain of the parameters in the analytical fitting procedure to that part of the parameter space where the analytical results correspond to the numerically integrated distributions [13].
- iii)* We have not yet included the effects of the Bose-Einstein statistics into the fitting, and finally
- iv)* We currently realized that the  $\chi^2$  hypersurface has a rather complicated shape when comparing our models to NA44 pion and kaon data. We hope that

the distinction among the various almost degenerate but physically different minima can be improved in the near future by including data on heavier particles into the data analysis.

The final results of the data analysis, to be obtained by eliminating the problems in items *i) - iv)*, will be reported elsewhere.

With the reservations as listed above, we have found the parameter values, summarized in Table 1, by applying the CERN MINUIT multidimensional fitting algorithm to determine the lowest values of  $\chi^2/NDF$  in the parameter space of the model. When we fit to pion data separately or only to kaon data, separately, we do not find a fit which were statistically better than the simultaneous fit to both the pion and kaon sample, see Table 2. The overall  $\chi^2/NDF$  does not change.

**Table 1.** Fitting HBT radius parameters and spectra from the model with analytical approximations, where the domain of the validity of the approximations is not taken into account, and with the numerically integrated radius parameters and spectra.

	Analytical (preliminary errors)	Numerical (preliminary errors)
$\chi^2/ndf$ , full fit	207/126	237/126
$\Delta\chi^2/bins$ , low $p_t$	77/42	104/42
$\Delta\chi^2/bins$ , high $p_t$	78/35	76/35
$\Delta\chi^2/bins$ , kaon	41/51	40/51
$\Delta\chi^2/bins$ , radii	12/9	18/9
$T_0$ [MeV]	$140 \pm 2$	$108 \pm 10$
$\tau_0$ [fm/c]	$4.6 \pm 0.2$	$7.0 \pm 0.5$
$R_G$ [fm]	$7.0 \pm 1.1$	$4.4 \pm 0.2$
$\Delta\eta$	$2.5 \pm 1.3$	$1.5 \pm 0.6$
$\Delta\tau$ [fm/c]	$3.2 \pm 1$	$2.4 \pm 1.3$
$f$	$0.89 \pm 0.03$	$0.88 \pm 0.12$
$b^2$	$0.52 \pm 0.08$	$0.68 \pm 0.14$
$d^2$	$499 \pm 50$	$130 \pm 8$

In Fig. 1 we show the result of the fit with the analytical expressions, displayed by a dashed line. The measured data points together with their error bars are also shown. Parameters  $a$  and  $b$  appear in a combined manner in the analytic expressions for the invariant momentum distribution, that is why the new variable  $f = b^2/(a^2 + b^2)$  is introduced in the fit.

The analytical formulas give a slightly better adjustment to the data than the description obtained by the numerically integrated emission function. This may either indicate that the analytical fit develops a fake minimum, or alternatively that some physics appears effectively in the analytic approximations which was

still missing from the emission function of eq. (1). The analytical formulas thus correspond to the source given by eq. (1) under certain restrictions only. A detailed numerical study indicated [13] that the conditions

$$\frac{r_{x,s}}{\tau_0} = \frac{\beta_t b R_*^2}{\tau_0^2 \Delta\eta_T^2} < 0.6$$

and  $\Delta\eta_*(y, m_t) < 0.9$  have to be satisfied simultaneously in order to reach less than 20 % relative error in the HBT radius parameters and the slope parameter of the IMD. This condition is violated by our analytic fit to the pion sample: from  $\frac{r_{x,s}}{\tau_0} < 0.6$  we obtain  $m_{t,\pi} < 200$  MeV, while from  $\Delta\eta_* < 0.9$  one obtains  $m_{t,\pi} > 300$  MeV, and these conditions cannot be satisfied simultaneously. The same conditions imply  $m_{t,K} < 600$  MeV, which is satisfied for the NA44 kaon data.

**Table 2.** Fitting either NA44  $\pi$  spectrum and radius parameters or  $K$  radius parameters and spectrum, with the numerically integrated model, in Boltzmann approximation.

	Only $\pi$ (preliminary errors)	Only $K$ (preliminary errors)
$\chi^2/ndf$ , full fit	195/76	40/48
$\Delta\chi^2/bins$ , low $p_t$	103/42	–
$\Delta\chi^2/bins$ , high $p_t$	75/35	–
$\Delta\chi^2/bins$ , kaon	–	40/51
$\Delta\chi^2/bins$ , radii	16/6	0/3
$T_0$ [MeV]	$112 \pm 2$	$133 \pm 6$
$\tau_0$ [fm/c]	$6.6 \pm 0.3$	$6.4 \pm 0.4$
$R_G$ [fm]	$4.1 \pm 0.1$	$12 \pm 1$
$\Delta\eta^2$	=2.2	=2.2
$\Delta\tau^2$ [fm <sup>2</sup> ]	=5.5	=5.5
$f$	$1.0 \pm 0.2$	$0.52 \pm 0.1$
$b^2$	$0.532 \pm 0.02$	$0.58 \pm 0.02$
$d^2$	=130	=130

Note that the restrictions given by the IMD data points, which do not yet have the systematic errors, seem to be so strong that the HBT  $m_t$ -dependent radius parameters from the fit are forced to deviate from the  $R_L \simeq R_{side} \simeq R_{out} \propto 1/\sqrt{m_t}$  rule, which is well satisfied by the NA44 data points. If we do tried not to fit the IMD of pions and kaons, our model were able to perfectly fit the 9 NA44 HBT data points, with large allowed region for the geometrical source sizes.

On this basis we expect that the inclusion of the systematic errors for the IMD of pions and kaons will improve the agreement between the model and the data. Note, however, that a fit to the measured particle spectrum is rarely obtained in such a good quality as obtained here. The fit with numerical integration is shown



on Fig. 1 with a full line. The  $\chi^2$  of the fit is somewhat high but still acceptable. The fit with the analytical formulas is shown on Fig. 1 with a dashed line. The difference between the two fits is only seen in the low  $p_t$  region for the pions.

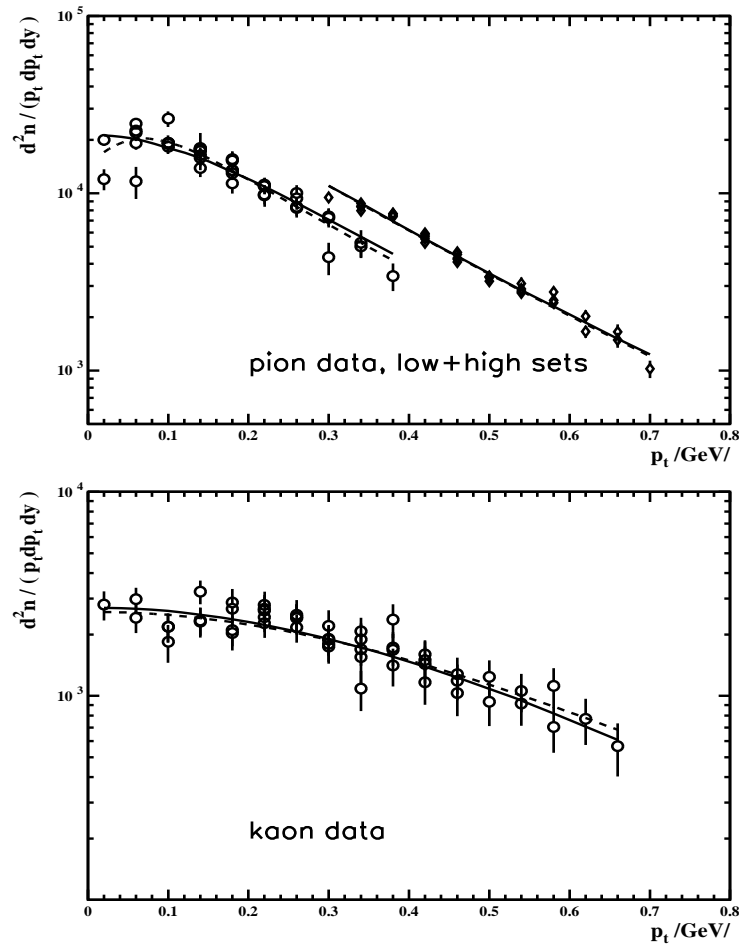


**Fig. 1.** The upper half shows the two pion IMD, the lower half the kaon IMD. Data are here displayed versus  $p_t$  and they are unnormalized. The full line shows the result of the fit with numerical integration, the dashed line the result using the analytical formulas. The rapidity of the data points is not shown. The acceptance is restricted to a small region in rapidity which changes with  $p_t$  specially for the pion data [2]. More than one data point for a  $p_t$  means neighbouring rapidity bins. The rapidity of the pions varies from 4.0 to 2.6, the rapidity of kaons spans 3.4 to 3.1. Data points at the edge of acceptance are not used.

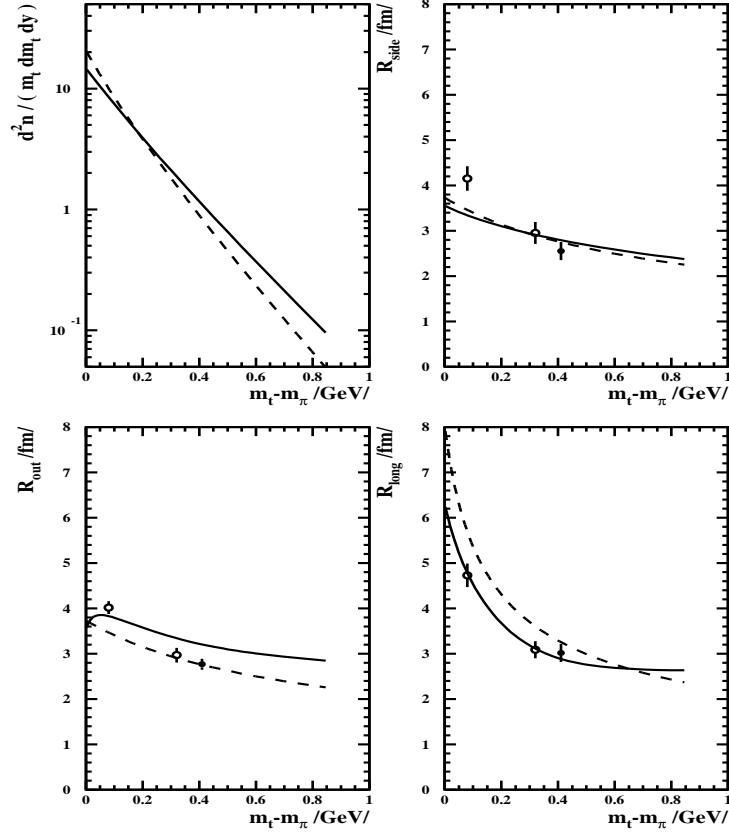


**Fig. 2.** Full line shows the fit using the numerical integration, dashed line shows the result of the analytical formulas with the parameters of the same fit. Data points are the radii measurements of NA44 [2]. Unfilled circles are used for pion data, filled for kaon data.

Fig. 2 shows the fit with numerical integration to the radii parameters and also the difference between the numerical integration and the analytical calculation using the parameters of the fit with numerical calculation. We see important differences mainly for the IMD. The radius parameters are reproduced by the analytic expressions with less than 20 % relative error at the transverse mass of the data points, and the slope parameters of the IMD for the pions is also reproduced up to a 20 % relative error.

When we fit the analytical formulas without restricting their domain of validity, the results are given in Table 1. Unfortunately, those parameter values which correspond to the best description of the data by the analytical formulas are outside of that region of the parameter space, where the analytic approximations correspond to the numerically evaluated emission function. Either the model emission function needs to be further adjusted in such a manner that its numerically integrated spectrum and HBT radius parameters will closely correspond to the presently found analytical formulas, or, if the emission function is fixed at its present form, one should not allow for fitting the data with the analytical formulas in an unrestricted domain of the parameter space. A more detailed analysis is needed, which can take into account that the errors of the analytic formulas increase strongly if we leave the domain of the 20% relative errors. This domain is given by the requirements  $\frac{r_{p,s}}{\tau_0} \leq 0.6$  and  $\Delta\eta_* < 0.9$ , see Ref. [13] for further details.

The fit implies that the model parameters  $a$ ,  $b$  and  $d$  take values significantly different from 0, approximately 0.3, 0.8 and 11, respectively.

## 4. Conclusions

This hydrodynamical model gives a fair description of data.

The analytical approximations provide less than 20% relative error for the HBT radius parameters and the slope parameters of the spectra in that part of the parameter space where the NA44 data are.

If we fit the approximative analytic results to data without estimating the errors of the approximations in the region, where the fit is performed, we find a fake minimum, where the extrapolated analytic results give a very good description of the data. However, at this part of the parameter space, no minimum is found when numerical integration is invoked. We find no evidence for different model parameters for pions or for kaons.

In a preliminary analysis, we find a surprisingly low central temperature at the mean time of the last interactions,  $T_0 = 108 \pm 10$  MeV. This is in agreement with our preliminary results presented at Quark Matter'95 [7]. Note that a similar low value of  $T_0 = 92.9 \pm 4.4$  MeV has been found at AGS energies from a detailed analysis of the BECF and the spectrum of both pions and kaons [14]. However, we would like to be careful and not to draw very strong conclusions until we can find a very well defined minimum by adding more data, utilizing the experimental estimate of the systematic errors on the spectrum, and until we have included the effects of quantum statistics on the single-particle spectra into the data analysis.

## Acknowledgement

One of us (B.L.) wants to thank the organizers for the invitation to this very stimulating workshop.

## Notes

- a. E-mail: csorgo@sunserv.kfki.hu
- b. E-mail: bengt@quark.lu.se

## References

1. T. Csörgő and B. Lörstad: hep-ph/9509213, *Phys. Rev. C* **54** (1996) 1390.
2. H. Beker et al., NA44 Collaboration, *Phys. Rev. Lett.* **74** (1995) 3340.
3. Michael Murray, NA44 Collaboration, private communication.
4. T. Csörgő, B. Lörstad, J. Zimányi, hep-ph/9411307, *Z. Phys. C* **71** (1996) 491.
5. J. Bolz, U. Ornik, M. Plümer, B. R. Schlei and R. M. Weiner, *Phys. Rev.* **D47** (1993) 3860.
6. S. Chapman, P. Scotto and U. Heinz, *Heavy Ion Physics* **1** (1995) 1; *Phys. Rev. Lett.* **74** (1995) 4400.
7. T. Csörgő and B. Lörstad, *Nucl. Phys.* **A590** (1995) 465c.
8. S. V. Akkelin and Yu. M. Sinyukov, Bogoljubov Institute Report No. ITP - 63 -94E, December 1994 (unpublished).
9. T. Csörgő and S. Pratt, Report No. KFKI - 1991 -28/A, p. 75 (1991).
10. This was not seen in Ref. [15], where it was assumed that pions and kaons are characterized by the same emission function.
11. M. Murray, NA44 Collaboration, *Heavy Ion Physics* **4** (1996) 213.
12. N. Xu, NA44 Collaboration, *Heavy Ion Physics* **4** (1996) 263.
13. T. Csörgő, P. Lévai, B. Lörstad, hep-ph/9603373, *Acta Phys. Slovaca* **46** (1996) 585.
14. S. Chapman and J. Rayford-Nix, Report No. LA-UR-96-0782.
15. U. Heinz, B. Tomásik, U. A. Wiedemann and Wu Y.-F., *Heavy Ion Physics* **4** (1996) 249.
16. J. Zimányi, T. S. Biró, T. Csörgő, P. Lévai, *Heavy Ion Physics* **4** (1996) 15.